

Systematic Definition of Protein Constituents along the Major Polarization Axis Reveals an Adaptive Reuse of the Polarization Machinery in Pheromone-Treated Budding Yeast

Rammohan Narayanaswamy,^{†,||,⊥} Emily K. Moradi,^{†,§,||,#} Wei Niu,^{†,||,▽,#} G. Traver Hart,^{†,||,#}
Matthew Davis,^{†,||,○,#} Kriston L. McGary,^{†,||,#} Andrew D. Ellington,^{*,†,‡,||} and
Edward M. Marcotte^{*,†,‡,||}

Center for Systems and Synthetic Biology, Departments of Chemistry and Biochemistry, and Biomedical Engineering,
Institute for Cellular and Molecular Biology, 2500 Speedway, University of Texas, Austin, Texas 78712

Received July 11, 2008

Polarizing cells extensively restructure cellular components in a spatially and temporally coupled manner along the major axis of cellular extension. Budding yeast are a useful model of polarized growth, helping to define many molecular components of this conserved process. Besides budding, yeast cells also differentiate upon treatment with pheromone from the opposite mating type, forming a mating projection (the 'shmoo') by directional restructuring of the cytoskeleton, localized vesicular transport and overall reorganization of the cytosol. To characterize the proteomic localization changes accompanying polarized growth, we developed and implemented a novel cell microarray-based imaging assay for measuring the spatial redistribution of a large fraction of the yeast proteome, and applied this assay to identify proteins localized along the mating projection following pheromone treatment. We further trained a machine learning algorithm to refine the cell imaging screen, identifying additional shmoo-localized proteins. In all, we identified 74 proteins that specifically localize to the mating projection, including previously uncharacterized proteins (Ycr043c, Ydr348c, Yer071c, Ymr295c, and Yor304c-a) and known polarization complexes such as the exocyst. Functional analysis of these proteins, coupled with quantitative analysis of individual organelle movements during shmoo formation, suggests a model in which the basic machinery for cell polarization is generally conserved between processes forming the bud and the shmoo, with a distinct subset of proteins used only for shmoo formation. The net effect is a defined ordering of major organelles along the polarization axis, with specific proteins implicated at the proximal growth tip.

Keywords: Proteomics • polarized growth • subcellular localization • pheromone response • yeast

Introduction

Polarizing cells undergo widespread molecular rearrangements in a spatially and temporally concerted manner, reorganizing cellular components along the primary cellular polarized growth axis. Polarization mechanisms are important for both basic cell division and specialized growth processes, such as formation of neuronal processes,¹ cell motility² and asym-

metric stem cell differentiation.³ The resultant coordinated asymmetry affects major developmental, cell division, and metabolic programs in the cell. The budding yeast, *Saccharomyces cerevisiae*, has proved an excellent model system for studying polarized growth, as it restructures the cell differentially in vegetative growth, mating and filamentous growth.⁴ Each of these developmental fates is characterized by a distinct morphology, and the stimulus and outcomes of each differentiation pathway are unique. For example, internal bud cues from the previous bud site drive the cycle of bud emergence and cytokinesis. External cues such as mating pheromone and nutrient starvation trigger signal transduction pathways that induce formation of a mating projection or the filamentous 'foraging' phenotype, respectively. These changes in cellular morphology are accompanied by dynamic changes in the cellular proteome that function in setting up the polarization axis and orchestrating specific activities required for the appropriate growth response.

* To whom correspondence should be addressed. E-mail: (E.M.M.) marcotte@icmb.utexas.edu, (A.D.E.) andy.ellington@mail.utexas.edu.

† Center for Systems and Synthetic Biology, University of Texas.

‡ Institute for Cellular and Molecular Biology, University of Texas.

§ Current address: Department of Pathology, Yale University School of Medicine, 310 Cedar Street LH 214, P.O. Box 208023, New Haven, CT 06520-8023.

⊥ These authors contributed equally.

|| Department of Biomedical Engineering, University of Texas.

○ Current address: Department of Molecular, Cellular, and Developmental Biology, KBT 926, Yale University, P.O. Box 208103, New Haven, CT 06620-8103.

▽ Current address: QB3 Institute, 387 Stanley Hall # 3220, University of California, Berkeley, CA 94720-3220.

Department of Chemistry and Biochemistry, University of Texas.

typified by the formation of a mating projection (the 'shmoo') accompanied by cell cycle arrest in the G1 phase (reviewed in refs 4 and 5). Many proteins are redistributed to different subcellular locations culminating in the formation of a highly structured polarization axis oriented toward the shmoo tip. Although similar polarization mechanisms dominate the formation of a bud and a mating projection, there are obvious differences underlying the two processes. While budding is preordained by location of the previous budding landmark, mating projection formation appears to be a dynamic process that relies in the wild on a directional pheromone gradient. Mating-competent cells can therefore continuously sense pheromone gradients and alter the site of projection formation accordingly, and in some instances, even sequentially form multiple 'shmoos'.⁴ Cells subjected in the laboratory to uniform pheromone concentrations form randomly oriented mating projections. The shape and structure of mating projections also differ from buds, with the conspicuous constriction that marks buds being largely absent at the base of the 'shmoos'. This region contains the septins, chitin, and pheromone induced proteins such as Afr1p that interact with the septins. It is therefore likely that an altered set of protein interactions during the mating process determines the shape and morphology of the projection and distinguishes it from bud formation during vegetative growth. This is more evident when one analyzes finer details such as the growth dynamics of a bud relative to a shmoo. Bud growth becomes isotropic after the apical growth phase, while a shmoo displays more unidirectional growth dynamics, possibly because of differential rates of recruitment of proteins that deposit cell wall constituents. These differences arise due to the distinct functional goals that each process seeks to achieve—nuclear segregation to the daughter and cytokinesis during vegetative growth, as opposed to cell fusion and karyogamy during mating.⁴ Systematic identification of the proteins associated with each process will therefore begin to shed light on their mechanistic differences.

Significant strides have been made in technologies for increasing the throughput of imaging protein spatial localization in mammalian cells (e.g., see refs 6 and 7), but the power of yeast genetics has already resulted in proteome-wide imaging and epitope tagging strategies being successfully employed in this model organism. Cellular imaging of protein localization has been conducted on transposon-tagged⁸ as well as recombination-based tagged open reading frame (ORF) libraries.⁹ Immunofluorescence and live-cell imaging of the tagged strains in *S. cerevisiae* has identified the subcellular localization of most of the proteome under standard laboratory conditions and these data are now accessible through the TRIPLES, GFP/UCSF, and other databases.

We previously reported the development of spotted cell microarrays¹⁰ (cell chips) for measuring cell morphology and morphology defects across collections of thousands of yeast strains, more recently applied to measure a bacterial protein's localization in thousands of differing genetic backgrounds.¹¹ Briefly, spotted cell microarrays allow for cells of different genetic backgrounds to be robotically arrayed onto coated glass slides at high density, then each strain imaged in turn using automated microscopy. The cell microarray approach is readily adapted to measure eukaryotic protein subcellular localization by taking advantage of the availability of epitope-tagged strain collections, such as the green fluorescent protein (GFP)-tagged strain collection.⁹ In this strain set, each of the ~4200 *S. cerevisiae* strains carries a genomic copy of the *Aequoria victoria*

GFP (S65T) gene fused to the carboxy-terminus of a different open reading frame. Arraying this strain set on spotted cell microarrays and imaging the entire set of strains thus measures the subcellular localizations of ~4200 proteins in parallel, providing a measure of each tagged protein's localization under the assayed conditions. This approach might logically be combined with immunofluorescence experiments, as a major advantage of the cell chips is the minimal use of expensive reagents on the chips, achieved by limiting the use of antibodies and dyes to single microscope slides. Imaging entire libraries on chips also results in reduced imaging times in comparison to, for example, imaging the 50 96-well plates required for the complete GFP tagged collection.

In this study, we have attempted to map the changes in localization of the yeast proteome upon formation of a mating projection. Although individual proteins that localize to the shmoo tip have been characterized (e.g., the shmoo tip marker Fus1¹²), proteome-wide screens have not been performed to measure such localization changes due to their expensive and cumbersome nature. We developed and implemented a cell microarray-based imaging assay for measuring the spatial redistribution of a large fraction of the yeast proteome, and applied this assay to identify proteins localized along the mating projection following pheromone treatment. By further incorporating information about known yeast gene associations and about protein localization during vegetative growth, we trained a machine learning algorithm to refine the cell imaging screen, resulting in a total of 74 proteins identified that specifically localize to the mating projection. Functional analysis of these proteins, coupled with analyses of individual organelle movements during shmoo formation, suggests a model in which the basic machinery for cell polarization is generally conserved between processes forming the bud and the shmoo, with a distinct subset of proteins used only for shmoo formation. The net effect is a defined ordering of major organelles along the polarization axis, with specific proteins implicated at the proximal growth tip.

Materials and Methods

Yeast Green Fluorescent Protein (GFP) Tagged Strains and Growth Conditions. Spotted cell microarrays were manufactured from the *S. cerevisiae* GFP tagged clone collection (Invitrogen), in which each of ~4200 individual strains with genetic background EY0986 (ATCC 201388: MAT α his3Δ1 leu2Δ0 met15Δ0 ura3Δ0 (S288C)) was chromosomally tagged with the coding sequence of *A. victoria* GFP (S65T) at the carboxy-terminal end of an open reading frame.⁹ This collection was copied in 96 well plates using a Biomek FX liquid handling robot, inoculating each strain into 200 μ L of YPD containing 17% glycerol, growing at 30 °C for ~2 days without shaking, mixed on a plate shaker, and sealed and frozen at -80 °C.

Alpha Factor Treatment. GFP-tagged strains were treated with alpha factor in the following manner: A copy of the GFP clone collection was thawed from -80 °C and a 1% inoculum used to seed a fresh copy in YPD medium. After growth to near saturation for ~36 h at 30 °C, this intermediate copy was used at 1% to inoculate another such one in YPD. This copy was grown overnight at 30 °C and was washed three times to inactivate secreted extracellular Bar1p protease that degrades alpha factor. Subsequently, alpha factor was added to each sample well in the collection at 75 μ g/mL final concentration and allowed to incubate for ~3 h at 30 °C. The samples were

fixed using freshly prepared 2% formaldehyde for 1 h at 30 °C and the excess fixative was removed by three successive washing rounds of YPD containing 17% glycerol before resuspension in 100 µL of YPD plus 17% glycerol. These sample plates were stored at -80 °C or directly printed.

Slide Preparation, Printing and Imaging of Cell Microarrays. Cell microarrays were printed onto freshly treated poly-L-lysine coated slides *via* contact deposition of a suspension of yeast cells from the arrayed yeast collection using a DNA microarray spotting robot. Locations of cell spots were identified by scanning the freshly printed slides using a GenePix microarray scanner, then cells in each spot were imaged using an automated Nikon E800 fluorescence microscope and Photometrics Coolsnap CCD camera as in Narayanaswamy et al.,¹⁰ collecting DIC images and fluorescent images in the DAPI and GFP channels from each spot, on two replicate slides, for a total of ~16 000 microscope images per slide. Images were stored and analyzed using the Cellma cell microarray image database software.¹⁰ Two independent graders manually inspected the images, selecting strains in which the GFP-fusion protein showed punctate localization proximal to the shmoo tip. Manual follow-up assays were then performed in the absence of fixative two or more times on independent live cultures (biological replicates), requiring reproducibility of shmoo localization in all assays. Additional cell microarrays were printed and imaged from the GFP-ORF strain collection in the absence of pheromone, serving as a negative control for the localization. This set also allowed comparison of cell microarray-based localization measurements with those observed in the original analysis of the strain set.⁹ For all shmoo-tip localized proteins identified, our untreated controls matched the published localizations, but the proteins localized to the shmoo in the presence of pheromone in all (≥ 3) replicate analyses.

Doubly Tagged Strains for Organelle Analysis. Doubly fluorescent strains for colocalization were constructed by mating and tetrad dissection. Red fluorescent protein (RFP) tagged marker strains (EY0987; ATCC 201389: MAT α his3Δ1 leu2Δ0 lys2Δ0 ura3Δ0 (S288C)) for nine organelles and cellular structures (gift of the laboratory of Erin O'Shea) were mated with the FUS1-GFP strain (EY0986), and diploids selected on Lys(-) Met(-) media. After sporulation, tetrads were dissected and doubly fluorescent 'a' type yeast propagated.

Image Analysis. Quantitative image analysis was performed using custom MATLAB image processing software. Primary software features include background noise removal, cell region identification, cell boundary segmentation, and subcellular feature description. All fluorescent images underwent background noise removal which was accomplished through background image subtraction and median filtering to remove speckle noise. Yeast cells were identified by implementation of the Kittler and Illingworth automated thresholding method¹³ on composite images for each field of view. These composite images were created by stacking all fluorescent channels as well as a histogram-modified DIC image. Cell boundary segmentation was accomplished using a seeded watershed algorithm in which the cell seed was generated using a fluorescent image of the DAPI stained nuclei. When DAPI stain was not available, cell segmentation was performed manually through image annotation in ImageJ.¹⁴ To remove improperly segmented cells, automatic cell segmentation results were required to meet predefined minimum and maximum cell size restrictions.

Subcellular feature identification was accomplished using cell-by-cell automated thresholding on each of the fluorescent channels.

Still images of the RFP/GFP/DAPI labeled yeast following alpha factor exposure were analyzed as above. Yeast cells identified in the images were computationally reoriented along the axis between the center of fluorescence of the DAPI stained nuclei and the GFP labeled shmoo tip. These rotated cells were then stretched or compressed so that the distance between these two points was uniform for all cells. After these transformations, each cell in the still images was overlaid so that RFP labeled organelle localization could be visualized.

Classifier Construction. To minimize false negative observations from the high-throughput screen, we trained a *naïve* Bayesian classifier¹⁵ to identify additional shmoo-tip localized proteins. For the training set, we employed the proteins identified in the high-throughput screen. Classifier features were aggregated from data provided by the UCSF GFP screen⁹ and the functional gene network of Lee et al.^{16,17} The features collected for each gene were the sum of the gene's network log likelihood scores (LLS) to the set of training genes, the ratio of the sum of the gene's LLS scores to the training set genes divided by the sum of LLS scores to all other genes, protein abundance (molecules per cell), and cell location (using primary cellular location). All features were numeric values except location which was treated as a discrete estimator (e.g., binary flags for nucleus, bud neck, etc.). The classifier was implemented in Weka and applied to the set of 5804 yeast genes, either using all training genes as the training/test set or using 10-fold cross-validation (both gave similar results). The classifier proved reasonably predictive, with an area under a 10-fold cross-validated receiver-operator characteristic (ROC) curve of 0.843. At the score threshold selected for experimental validation, shmoo-localized proteins were predicted with a cross-validated true positive rate of 0.51 and a false positive rate of 0.027. This corresponds to recovering 20 of the 37 shmoo genes (cross-validation: 19). An additional 151 (cross-validation: 153) genes not identified in the initial screen were also classified as shmoo genes using a 0.5 probability cutoff. Of the 151 genes, 118 were present in the GFP library and were rescreened manually; 37 of these proved to be shmoo localized.

Results and Discussion

1. Organellar Movement during Pheromone-Induced Polarized Growth. It has been previously observed that organelles move during the pheromone-induced, polarized growth of yeast.¹⁸ To establish conditions for screening for genes involved in polarized growth, we used fluorescence microscopy to identify reproducible trends in organellar movements. We systematically measured the subcellular localization of 9 major organelles via organelle-specific fluorescent protein fusion markers. For each organelle, we constructed a yeast strain expressing both a red fluorescent protein (RFP)-tagged organelle marker, and an orientation marker, a green fluorescent protein (GFP)-tagged shmoo tip marker, Fus1. The positions of the two fluorescent protein markers and the nucleus (detected by staining with DAPI dye) were determined before and after treatment with the mating pheromone alpha factor. Image analysis was used to quantify each organelle's spatial distribution across >100 individual cells in an image (Figure 1). Organellar positions were calculated after reorienting and scaling each individual cell in the image to a common reference frame (the axis from the nucleus to the shmoo tip).

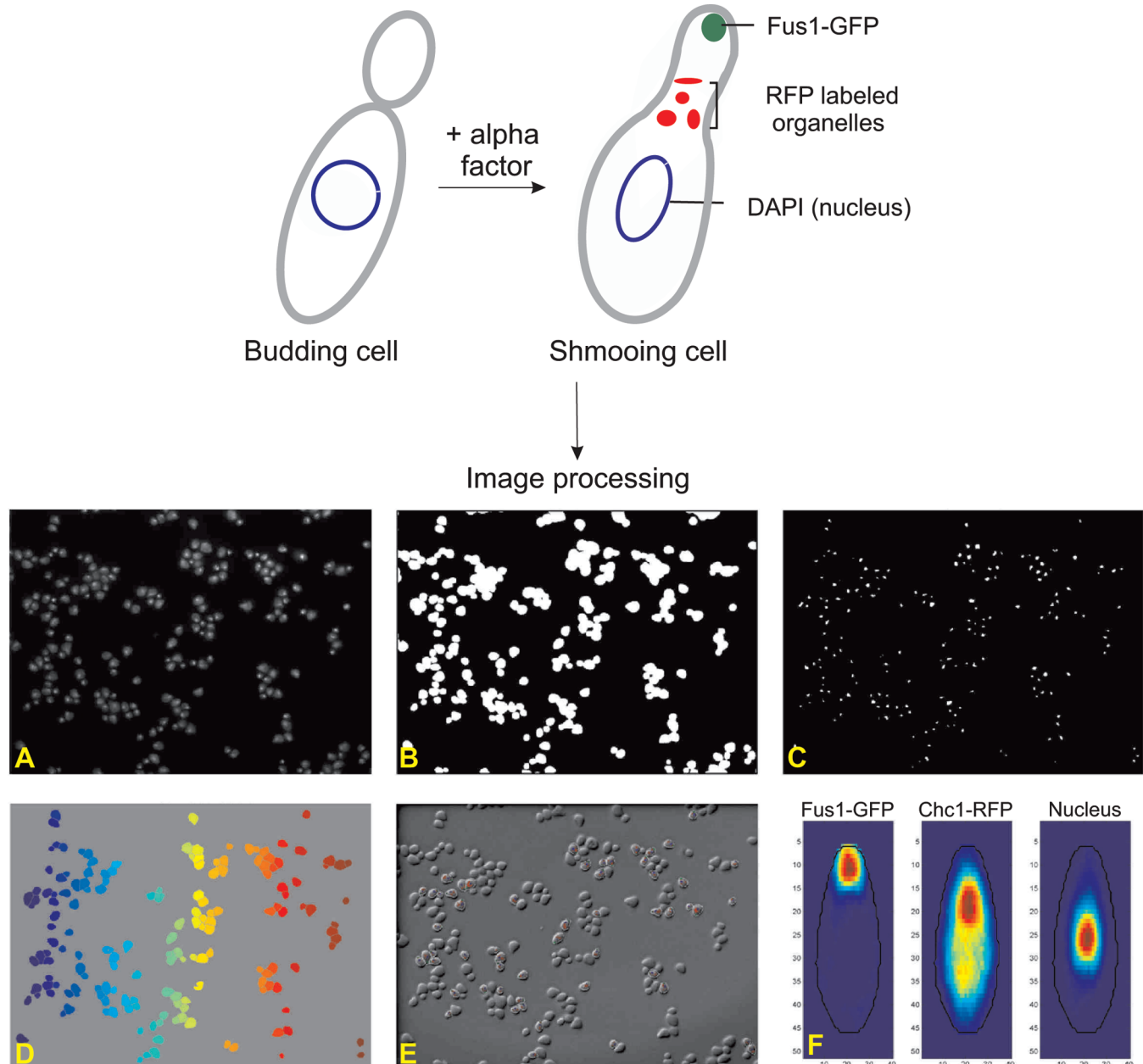


Figure 1. Protocol for quantifying organellar localization following pheromone treatment. Synthetic alpha factor was added to vegetatively growing cells containing GFP tagged Fus1 and one of nine different RFP tagged organellar marker proteins. Computational image analysis was used to measure the subcellular distribution of the tagged organellar marker as illustrated. (A) Image of shmoo tip marker Fus1 labeled with GFP, clathrin marker Chc1 labeled with RFP, cell nuclei stained with DAPI. (B) Binary thresholded image. (C) Binary image of nuclei used to seed watershed segmentation. (D) Result of watershed segmentation. (E) Shmoos were identified and cell-by-cell thresholding on the Fus1-GFP, Chc1-RFP, and nuclear (DAPI) images was overlaid on the DIC image. (F) Result of rotating and overlaying thresholded fluorescent intensity distributions for all shmoos ($n = 324$) from multiple still images, measuring the distribution of the RFP-tagged organellar protein (here, Chc1) throughout the observed cells and plotted relative to the shmoo tip and nuclear markers. In this case, clathrin (as localized by Chc1) shows a definite bias toward the shmoo tip and lies predominantly between the shmoo tip and nucleus.

Each organelle marker strain (Figure 2) strongly revealed the formation of an axis of polarity, presumably toward the pheromone gradient in anticipation of the mating process and subsequent cellular fusion. Several common features about organellar arrangement were evident: The nucleated actin filaments that form the actin cables were polarized toward the shmoo tip (as evidenced by Sac6-RFP fusions, the cross-linking fimbrin protein used as the marker). This was consistent with actin cables acting as ‘conduits’ for transporting organelles during mating, just as they do during vegetative growth.⁴ The

spindle pole body core component, Spc42, was prominent in its movement toward the shmoo tip, indicating that the tethered spindle microtubules, the nuclear envelope and the chromosomes were also reoriented.^{18,19} In consequence, the entire nucleus was also reoriented toward the shmoo tip, with the nucleolus being preferentially located at the opposite side of the nucleus relative to the shmoo tip. Another consequence was extensive vesicular trafficking of cargo intended for membrane deposition and new cell wall formation at the site of the shmoo projection (as evidenced by localization of

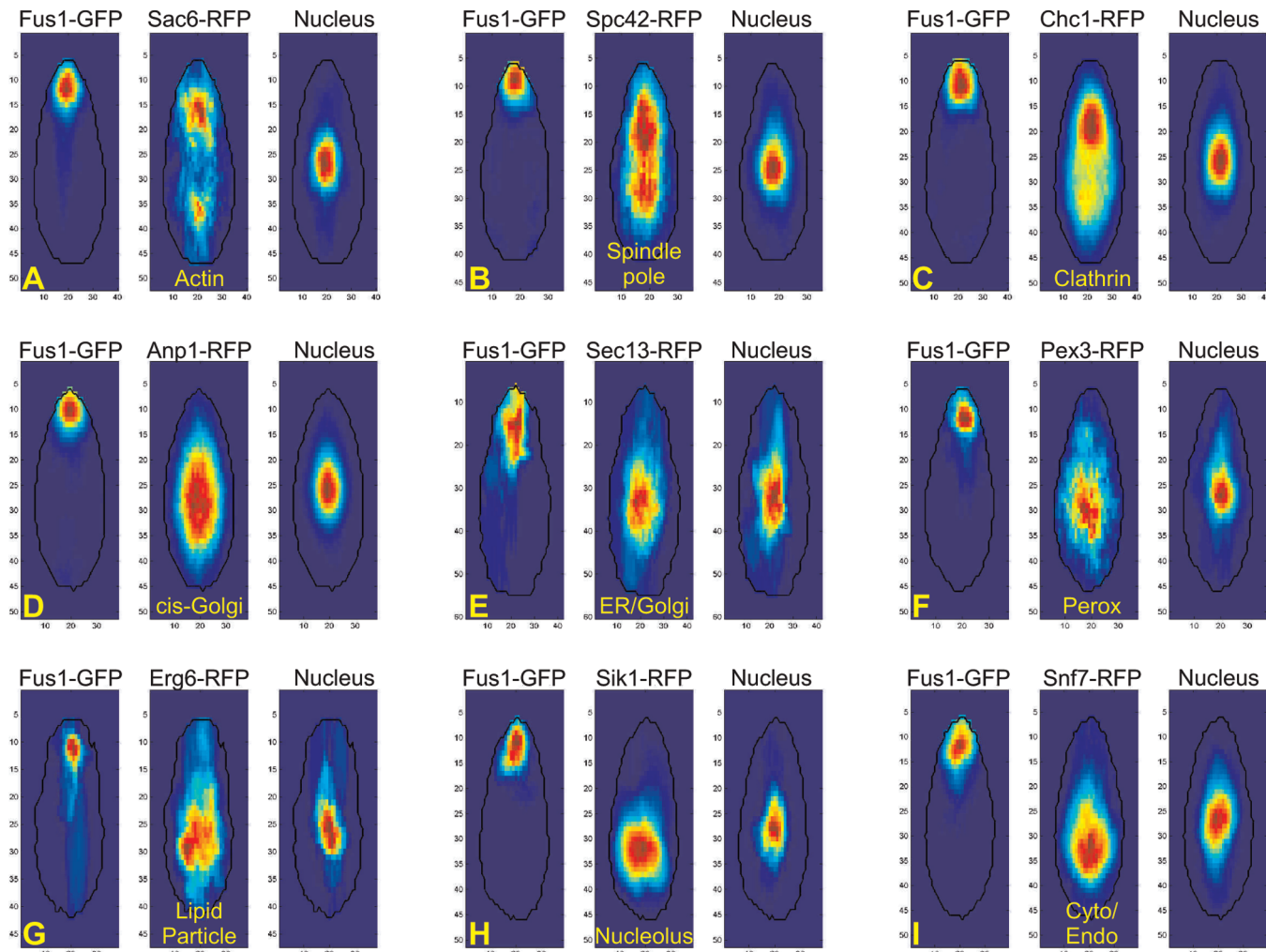


Figure 2. Organelles are differentially distributed along the polarization axis. Results of rotating and overlaying thresholded fluorescent intensity distributions for all shmooring cells from multiple still images are shown for each of nine organellar markers. Each triptych shows a shmooring tip marker (FUS1) labeled with GFP, the indicated organelle marker labeled with RFP, and the cell nuclei stained with DAPI. (A) Actin, SAC6, (B) spindle pole, SPC42, (C) clathrin, CHC1, (D) golgi cis-cisterna, ANP1, (E) ER/golgi, SEC13, (F) peroxisome, PEX3, (G) lipid particle, ERG6, (H) nucleolus, SIK1, and (I) cytoplasm/endosomal membranes, SNF7.

clathrin protein Chc1 with Fus1-GFP). No bias toward the polarization tip was observed for the endoplasmic reticulum marker Sec13, a component of the Nup84 nuclear pore complex and COPII complex. As expected, there was a broad distribution of a Golgi cisternal marker, Anp1, both toward and away from the shmooring tip. While polarization was along the shmooring tip axis, transport may occur in both directions. The endosome marker, Snf7 tended to accumulate away from the shmooring tip, possibly implicating the involvement of the endocytic pathway in trafficking components between the membrane and the vacuole (for example, the pheromone receptor Ste2 which upon pheromone binding and ubiquitination, is internalized and endocytosed into vesicles).²⁰ Analysis of yeast expressing the GFP-tagged mitochondrial marker Ilv3 (data not shown) revealed mitochondria throughout the shmooring cells, occasionally shmooring tip localized but also generally found widely distributed.

Overall, our results are consistent with the establishment of an alpha factor-induced polarization axis which leads to the spatial reorganization of multiple organelles in a roughly

ordered fashion from proximal to the shmooring tip to the distal end of the cell.

2. Identification of Specific Proteins and Pathways Contributing to Polarized Growth. Having established a reproducible cell-by-cell organellar reorganization along the polarization axis, we attempted to identify the numerous proteins and protein complexes that mediated these cell-wide changes in morphology and distribution. We therefore undertook a systematic, high-throughput analysis of alpha factor-induced changes in protein localization of GFP-tagged yeast strains. It should be noted that a comprehensive survey of proteins localized to the shmooring tip has not previously been carried out despite many studies^{21–24} that have implicated key roles for individual proteins in this dynamic cellular compartment. Building on our previous success in constructing and screening yeast cell microarrays,¹⁰ we screened the collection of GFP-tagged yeast strains for pheromone-induced changes in protein localization.

2.1. Identifying Pheromone-Induced Changes in Protein Localization Using Cell Microarrays. An overview of the cell microarray assay is presented in Figure 3. Briefly, after treating

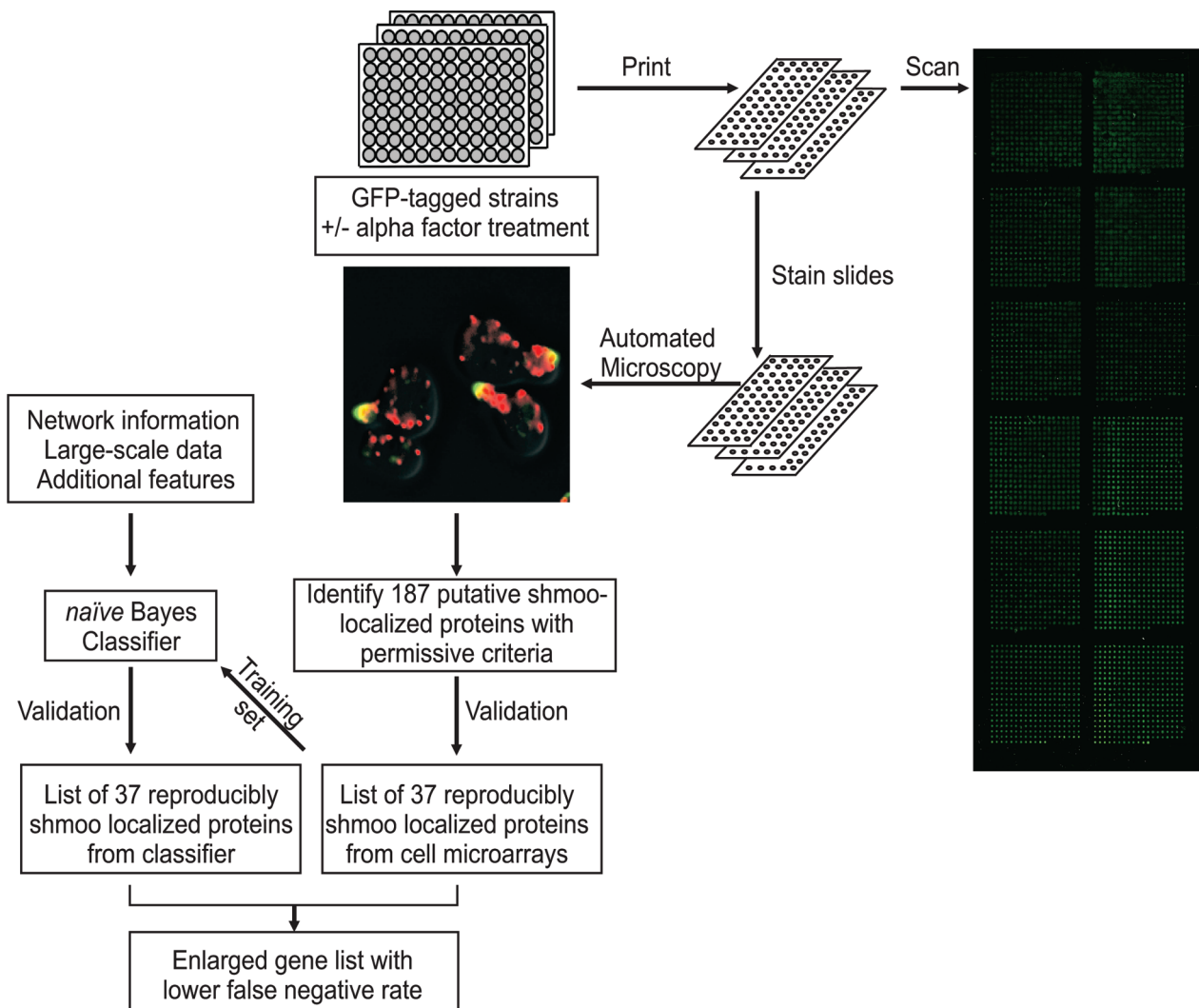


Figure 3. Schematic of the work flow for performing the proteome-wide localization screen. The GFP tagged yeast library was treated with mating pheromone, the cells were fixed, and then microarrayed onto a microscope slide. High-throughput microscopy of the arrayed strains revealed proteins localized to the polarized growth tip. This gene set was expanded by training a machine learning classifier to distinguish the observed proteins from the rest of the proteome on the basis of their vegetative expression patterns⁹ and their connections in a functional gene network.¹⁷ Additional proteins identified from the classifier were manually validated, resulting in a final set of 74 proteins localized to the polarized growth tip of the mating projection.

the library of GFP-tagged fusion protein expression strains with alpha factor, we fixed and robotically printed⁹ the strains onto poly lysine-coated microscope slides¹⁰ and imaged the fixed strains using automated microscopy. We screened for proteins showing a clear localization proximal to the shmoo tip. In all, 187 proteins were chosen from the initial screen, based on a lenient criterion that included even marginal examples. These 187 strains were then manually retested in the absence of fixative, which improved signal-to-noise value because of reduced background fluorescence. The follow-up screen yielded 37 strains in which GFP fusion proteins were consistently localized to the shmoo tip (Table 1).

Statistical analysis of the functions present²⁵ showed a significant enrichment for several pathways and processes, including genes involved in secretion/exocytosis, budding/cell polarity, cytoskeletal organization, and pheromone response/mating specificity. Representative examples are shown in Figure 4.

In contrast, of the 150 proteins not confirmed by the manual follow-up imaging assay, roughly 65% were either mitochon-

drial proteins or proteins that were localized at the shmoo neck or at the base of the shmoo tip. These classes were obviously difficult to distinguish from true proximal shmoo localization, leading to their inclusion in our initial lenient screen. The remaining 35% of the excluded proteins exhibited punctate structures not reproducibly associated with the shmoo tip (e.g., peroxisomal proteins). The high-throughput survey recovered about 15% of the SGD-annotated, shmoo-localized proteins (Figure 5, Table 1). This high false negative rate is likely due to fixation induced autofluorescence, which masks low-abundance proteins.

2.2. Computational Identification and Confirmation of Additional Shmoo-Localized Proteins. To reduce the high false negative rate, we took advantage of near genome-wide data sets of protein localization in vegetative growing yeast cells^{9,26} and an integrated probabilistic gene network^{16,17,27} of functional genomic and proteomics data in order to develop a machine learning algorithm for predicting additional proteins localized to the shmoo tip (for example, proteins that had been missed because of low expression or penetrance). As detailed

Table 1. Manually Verified Shmoo Tip Localized Genes Identified by the Cell Chip

gene name	ORF name	Human ortholog ^a	Gene Ontology biological process annotation
ABP1	YCR088W	DBNL	establishment of cell polarity (sensu Fungi)
AIP1	YMR092C	WDR1	response to osmotic stress
BEM3	YPL115C	-	pseudohyphal growth
CAP1	YKL007W	CAPZA2	barbed-end actin filament capping
CAP2	YIL034C	CAPZB	filamentous growth
CAR1	YPL111W	ARG1	arginine catabolism to ornithine
CBK1	YNL161W	STK38L	regulation of exit from mitosis
CDC10	YCR002C	SEPT9	cell wall organization and biogenesis
CDC11	YJR076C	-	cell wall organization and biogenesis
CDC48	YDL126C	VCP	ubiquitin-dependent protein catabolism
EDE1	YBL047C	EPS15	endocytosis
END3	YNL084C	-	endocytosis
ENT1	YDL161W	EPN3	endocytosis
EXO70	YJL085W	-	cytokinesis
EXO84	YBR102C	EXOC8	exocytosis
FUS1	YCL027W	-	conjugation with cellular fusion
INP52	YNL106C	SYNJ2	cell wall organization and biogenesis
KEL1	YHR158C	RABEPK	cell morphogenesis
LSG1	YGL099W	GNL1	ribosome biogenesis
MID2	YLR332W	-	cell wall organization and biogenesis
PEA2	YER149C	-	pseudohyphal growth
POP2	YNR052C	CNOT8	regulation of transcription from RNA polymerase II promoter
SEC10	YLR166C	EXOC5	establishment of cell polarity (sensu Fungi)
SEC18	YBR080C	NSF	ER to Golgi vesicle-mediated transport
SEC2	YNL272C	-	exocytosis
SEC3	YER008C	-	cytokinesis
SEC5	YDR166C	EXOC2	cytokinesis
SEC6	YIL068C	EXOC3	cytokinesis
SEC8	YPR055W	EXOC4	cytokinesis
SHM2	YLR058C	SHMT1	one-carbon compound metabolism
SHR3	YDL212W	-	ER to Golgi vesicle-mediated transport
SLA1	YBL007C	GRAP	cell wall organization and biogenesis
SLG1	YOR008C	-	cell wall organization and biogenesis
SMY1	YKL079W	-	exocytosis
YCR043C	YCR043C	-	biological process unknown
YMR295C	YMR295C	-	biological process unknown
YOR304C-A	YOR304C-A	-	biological process unknown

^a As calculated by InParanoid,⁵⁶ listing only the top-scoring inparalog.

in Materials and Methods, our initial set of 37 proteins obtained from the cell chip screen was used to train a *naïve* Bayesian classifier. Application of the classifier identified 151 proteins exceeding a 50% probability score threshold. An advantage of this approach is that the delimited set of candidate genes could then be individually assayed in the absence of fixative, a task that was greatly simplified because 118 of the 151 proteins were already present in the extant GFP library. We manually retested each of these 118 GFP fusion strains for protein localization to the shmoo tip. From this set, 37 additional proteins (~31%) were confirmed to be shmoo-localized (Table 2).

The classifier-guided retesting strategy doubled the coverage of the screen, and any remaining false negatives could be rationalized based upon low protein abundance. Of genes in the GFP library, we could identify 63% of the known shmoo tip-localized proteins that were present at >2500 molecules/cell, but less than 21% of known proteins with <2500 molecules/cell. On average, the shmoo tip proteins identified via the classifier method were less abundant than those recovered via the cell chip method lending credence to using a network guided approach to expand an initial list of seed genes. Although we were interested in specifically identifying proteins localized to the shmoo tip and therefore picked the highest confidence linkages, it must be mentioned that this process

might be iterated to potentially reveal more genes that are related to the pheromone response pathway.

3. Adaptive Reuse of Polarization Machinery. The 74 shmoo-tip localized proteins (37 from the cell microarray screen, 37 from computational prediction and screening) showed a marked enrichment for Gene Ontology functional categories related to polarized growth (with $p < 10^{-6}$ being the threshold of probability calculated using a hypergeometric distribution²⁸ that the intersection of given list with any functional category occurs by chance), with the strongest enrichment observed for the GO Biological Process annotation *establishment of cell polarity* ($p < 10^{-35}$), followed by annotations including *anatomical structure morphogenesis* ($p < 10^{-32}$), *cellular bud site selection* ($p < 10^{-29}$), *cytokinetic process* ($p < 10^{-28}$), *vesicle-mediated transport* ($p < 10^{-22}$), *reproduction* ($p < 10^{-20}$), *endocytosis* ($p < 10^{-18}$), *actin filament organization* ($p < 10^{-13}$), *exocytosis* ($p < 10^{-12}$), and *conjugation* ($p < 10^{-6}$). More specifically, we note that many of the proteins localized to the shmoo tip belong to protein complexes that are also involved in mediating polarized growth at the bud tip during vegetative growth (Figure 5). Thus, there appears to be broad adaptive reuse of the polarization machinery between these two processes. In addition, 41 of the 74 proteins have human

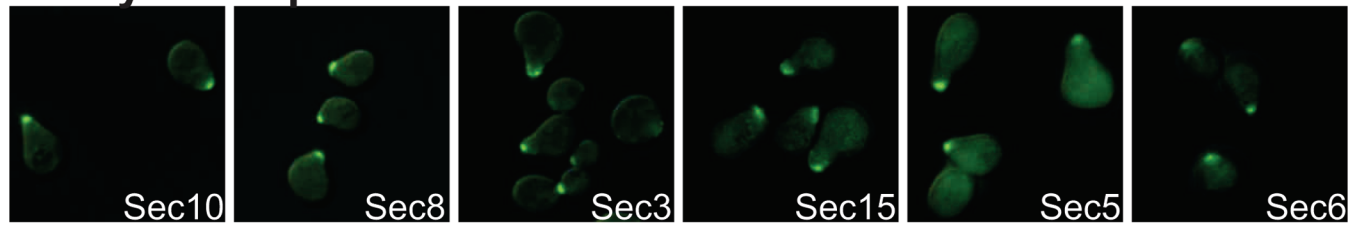
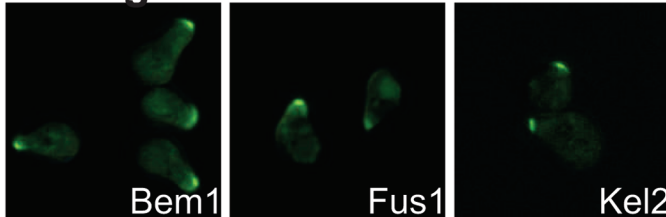
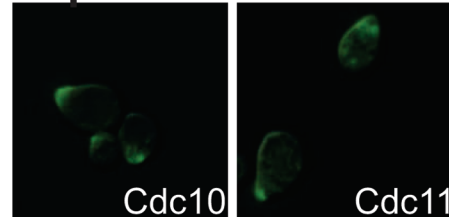
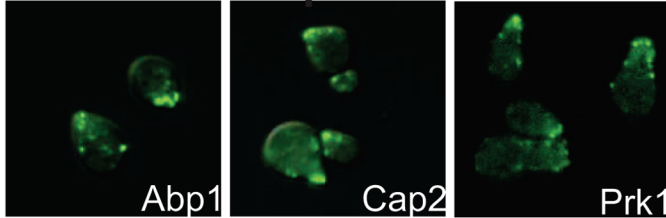
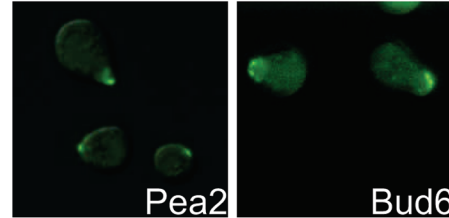
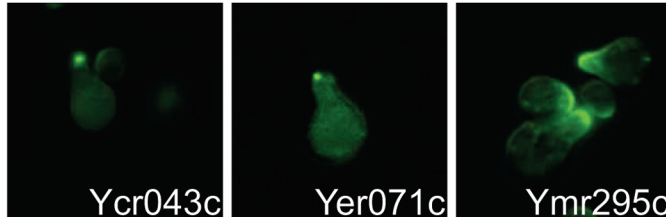
Exocyst complex**Mating****Septin****Actin cortical patch****Polarisome****Uncharacterized**

Figure 4. Representative components of cellular systems found localized to the shmoo tip. Each panel shows a few cells from one yeast strain expressing a GFP-tagged protein localized to the shmoo tip following pheromone response. Components of the exocyst were reconstructed almost in their entirety, along with many other relevant cellular systems (Tables 1 and 2), including proteins known to participate in mating, formation of the septin filaments and the actin cortical patches, and the polarisome. Proteins that function in signaling and fusion events such as Bem1, Fus1 and Kel1 were also represented, as were several otherwise uncharacterized proteins.

orthologs (Tables 1 and 2), indicating the general conservation of these processes across eukaryotes.

The exocyst is an evolutionarily conserved octameric protein complex thought to be targeted to the plasma membrane through the interaction of Exo70 with phospholipids²⁹ and stabilized by Sec3.³⁰ One of the major functions of the exocyst is to direct docking of myosin motor driven vesicles at the bud site during vegetative growth; the peripheral exocyst component Sec3 has also been previously implicated in pheromone-induced polarization.³¹ We show here that all 8 subunits of the exocyst localize to the shmoo tip (Figures 4 and 6), strongly supporting a conserved role in the polarization machinery of the two polarized growth processes.

The pentameric septin ring, a collar-like structure that is one of the first organizing components at the site of polarized growth, may also be localized at the shmoo neck,^{4,32} given that a number of its component proteins (Cdc10, Cdc11 and Shs1) were recovered in our screens (Figure 4). Cdc12, another septin

component, displayed filamentous structure and orientation toward the polarization axis. However, Cdc3, the fifth component, was absent from the GFP library, and thus could not be identified by either screen.

On a larger scale, there is clearly remodeling of the actin cytoskeleton and vesicular transport (to enable membrane and cell wall deposition) during shmoo formation,³³ and these proteins were heavily represented in our screens (Figures 4 and 6; Tables 1 and 2). Sac6, a fimbrin protein involved in bundling actin monomers to filaments, was localized at the shmoo tip, as was the twinfilin Twf1, a protein that assists in actin monomer localization to sites of rapid filament formation.³⁴ Twinfilin localization is assisted by the cap binding proteins Cap1 and Cap2,³⁴ which were also recovered in the screen. The dynamic nature of actin reorganization at the shmoo tip was indicated by the identification of Aip1, which is known to regulate cofilin mediated actin depolymerization.³⁵

Table 2. Manually Verified Shmoo Tip Localized Proteins Identified by the Classifier

gene name	ORF name	human ortholog ^a	Gene Ontology biological process annotation
ABP140	YOR239W	METTL2B	actin cytoskeleton organization and biogenesis
ARK1	YNL020C	AAK1	protein amino acid phosphorylation
BCK1	YJL095W	-	protein amino acid phosphorylation
BEM1	YBR200W	-	establishment of cell polarity (sensu Fungi)
BNI1	YNL271C	DIAPH1	pseudohyphal growth
BOI1	YBL085W	-	establishment of cell polarity (sensu Fungi)
BSP1	YPR171W	-	actin cortical patch distribution
BUD6	YLR319C	-	actin filament organization
BZZ1	YHR114W	TRIP10	endocytosis
CHS3	YBR023C	-	cytokinesis
CHS5	YLR330W	-	spore wall assembly (sensu Fungi)
ENT2	YLR206W	EPN3	endocytosis
KEL2	YGR238C	RABEPK	conjugation with cellular fusion
LAS17	YOR181W	WASL	endocytosis
MYO2	YOR326W	MYO5B	vesicle-mediated transport
MYO5	YMR109W	MYO1E	cell wall organization and biogenesis
PAN1	YIR006C	-	endocytosis
PRK1	YIL095W	AAK1	protein amino acid phosphorylation
RGD1	YBR260C	ARHGAP21	response to acid
RVS161	YCR009C	BIN3	endocytosis
RVS167	YDR388W	-	endocytosis
SAC6	YDR129C	PLS3	endocytosis
SEC15	YGL233W	EXOC6	cytokinesis
SEC31	YDL195W	SEC31A	ER to Golgi vesicle-mediated transport
SFB3	YHR098C	-	ER to Golgi vesicle-mediated transport
SHS1	YDL225W	-	establishment of cell polarity (sensu Fungi)
SLA2	YNL243W	HIP1R	actin filament organization
SMI1	YGR229C	-	regulation of fungal-type cell wall biogenesis
SRV2	YNL138W	CAP1	pseudohyphal growth
SYP1	YCR030C	-	biological process unknown
TWF1	YGR080W	TWF1	bipolar bud site selection
VRP1	YLR337C	WIPF1	endocytosis
WSC2	YNL283C	-	cell wall organization and biogenesis
WSC3	YOL105C	-	cell wall organization and biogenesis
YDR348C	YDR348C	-	biological process unknown
YER071C	YER071C	-	biological process unknown
YIR003W	YIR003W	-	biological process unknown

^a As calculated by InParanoid,⁵⁶ listing only the top-scoring inparalog.

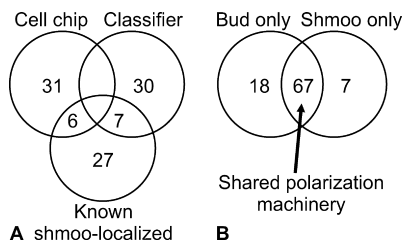


Figure 5. Venn diagram summarizing the proteins recovered. (A) Intersection of the cell chip and classifier identified proteins with the known set of shmoo tip localized proteins as annotated in the *Saccharomyces Genome Database*. (B) Of the 306 strains manually tested following either the cell chip or classifier, 18 were uniquely localized to the bud tip, 7 to the shmoo tip, and 67 to both.

The actin regulating kinases Ark1 and Prk1 were found and are known to modulate actin cortical patch components and endocytic pathways through phosphorylation cycles.^{36,37} Substrates of Ark1 and Prk1 that were recovered included Sla1, Sla2, Pan1, Ent1, and Ent2 suggesting the involvement of the Pan1-End3-Sla1p complex that is known to be required not only for actin cytoskeleton organization but also for normal cell wall morphogenesis.³⁸ Srv2, another tip-localized protein, binds

adenylyl cyclase and ADP-actin monomers and may facilitate regulation of actin dynamics and cell morphogenesis.³⁹

Consistent with the idea that Sla1 couples proteins in the actin cortical patch with the endocytic machinery,^{40,41} we observed cortical patch proteins such as Las17 (homologue of human Wiskott Aldrich syndrome protein), Vrp1 (homologue of human wasp interacting protein), Abp1 and Abp140 as well as proteins involved in endosomal vesicle trafficking, endocytosis and exocytosis at the shmoo tip. For instance, proteins such as Sfb3, Sec31 and Shr3^{42,43} mediate sorting of COPII vesicles between the ER and Golgi, and Sec18,⁴⁴ which is involved in post-Golgi vesicular transport. Other endosomal pathway proteins such as Bsp1 that functions as an adaptor linking the synaptojanin protein Inp52 implicated in TGN-to-early endosome sorting to the cortical actin cytoskeleton⁴⁵ were also identified. The type V myosin, Myo2 along with its interacting partners and cargo peroxisomes compose the observed vesicular transport phenomena directed at the shmoo tip. Myo2, for example, interacts with Chs5 to deliver chitin synthase enzyme Chs3 and with Smy1 to transport vesicles, and organelles such as vacuole⁴⁶ toward the tip. The final step involves docking and tethering of the endosomal vesicles to the site of polarized growth. Sec2,⁴⁷ a protein that functions as the Guanine nucleotide exchange factor for the rab GTPase

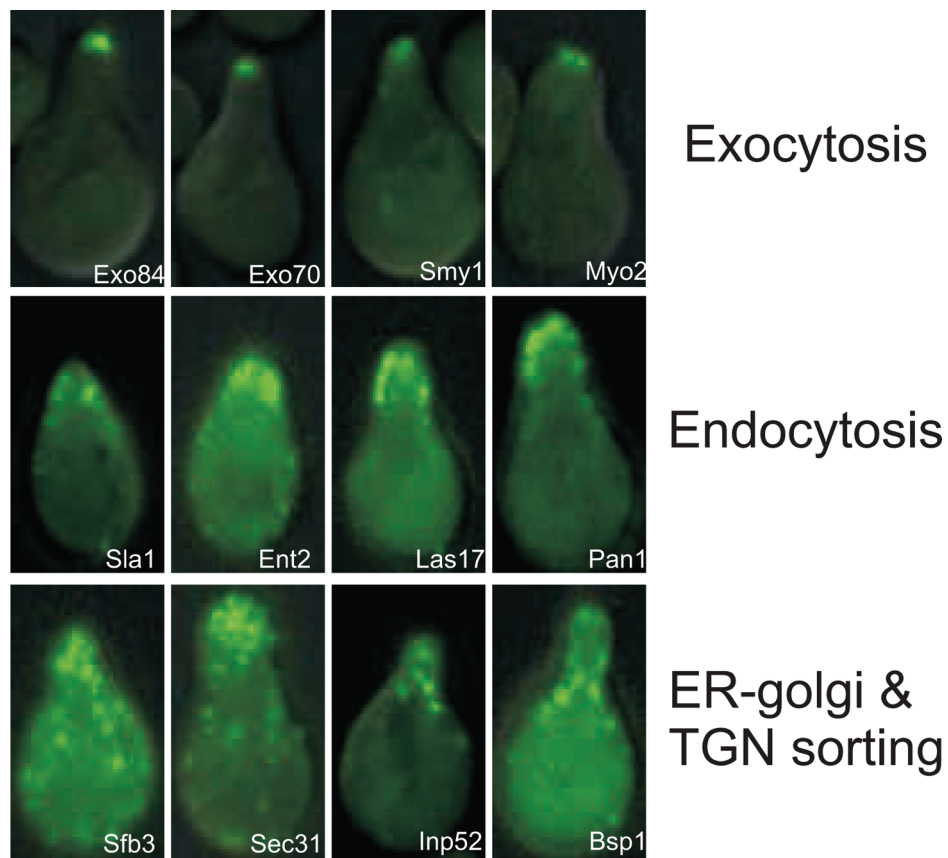


Figure 6. Spatially distinct localization of different vesicle transport processes is apparent along the shmoo tip. Several representatives of each process are shown. Proteins involved in exocytosis, including components of the exocyst, are tightly localized to the extreme tip of the shmoo. Proteins primarily involved in endocytosis are clustered along the shmoo tip proximal area, presumably indicative of endocytosis hot spots. Proteins that are part of other events such as ER-golgi and TGN vesicular sorting are notably more diffuse in their distribution, with a bias towards the shmoo tip. Proteins such as Inp52 and Bsp1 include components of the actin cortical patch machinery that directly interact with and serve as docking sites for the sorted cargo, but which nonetheless show a weaker bias towards the shmoo tip.

Sec4, mediates vesicle tethering to the exocyst and localizes at the shmoo tip. Proteins involved in cellular processes such as maintenance of cell wall integrity (Rgd1, Slg1, Wsc2, Wsc3) and in cell fusion (Kel1, Kel2 and Fus1) are tip localized as well as tying polarization events and pheromone specific functions at a systemic level.

An interesting observation made from the shmoo tip localization screen was the relative positioning of the proteins that were involved in various phases of vesicle mediated transport in our images (Figure 6). Proteins that were involved in exocytosis, such as the components of the exocyst, were spatially situated tightly at the shmoo tip as compared to the rest of the proteins from the screen. These proteins are involved in the final stages of protein transport such as protein docking and secretion and presumably indicate regions of membrane-vesicle interactions. In contrast, proteins of endocytosis localized more broadly around the shmoo tip, often with a punctate distribution possibly defining hot spots of endocytosis, and including proteins such as Sla1, Las17 and others. Formation of such hot spots is still an active area of research with recent discoveries being made in yeast of 'eisosomes' that appear to mark endocytic sites.⁴⁸ The actin cytoskeleton and cortical proteins play important roles in such processes with Rvs161 (also identified in this screen) interacting with eisosomal marker proteins.²⁷ Lastly, proteins involved in ER-Golgi and trans-Golgi to plasma membrane vesicle trafficking showed a definite bias of GFP signal toward the shmoo tip, presumably

reflecting vesicular transport, but were even more broadly distributed around the tip than the exocytic or endocytic proteins.

Several uncharacterized proteins recovered in our screen, such as Ymr295c,⁴⁹ Ydr348c, and Yor304c-a, localize to both the bud⁹ and shmoo tips suggesting a role in the general polarization machinery. Examination of these proteins' functional associations in the yeast functional gene network²⁷ provides some suggestions for their connection to particular aspects of polarized growth (Figure 7A): Yor304c-a is most tightly functionally associated with Bud6, a central protein in signaling polarization (also recovered in the screen) and Duo1, a cytoskeletal protein. Ymr295c and Ydr348c link to each other, with the former also strongly associated with glycolytic transcription factor Gcr1, and the latter associated with cell cycle progression genes Clb2 and Cdc28. This may suggest a role for these genes connecting polarization with processes such as cell cycle state and metabolism.

4. Proteins Unique to the Bud or Shmoo Tip. In addition to proteins playing a role in polarization during vegetative growth and mating, we identified a set of proteins that may be unique to one or the other process. Among the 81 false positive GFP-tagged strains predicted to be shmoo tip-localized by the classifier, several were involved in vesicular transport with 18 localizing to the bud tip (Figure 5). In other words, even though the computational method did not always directly predict localization to the mating tip, it predicted proteins involved in

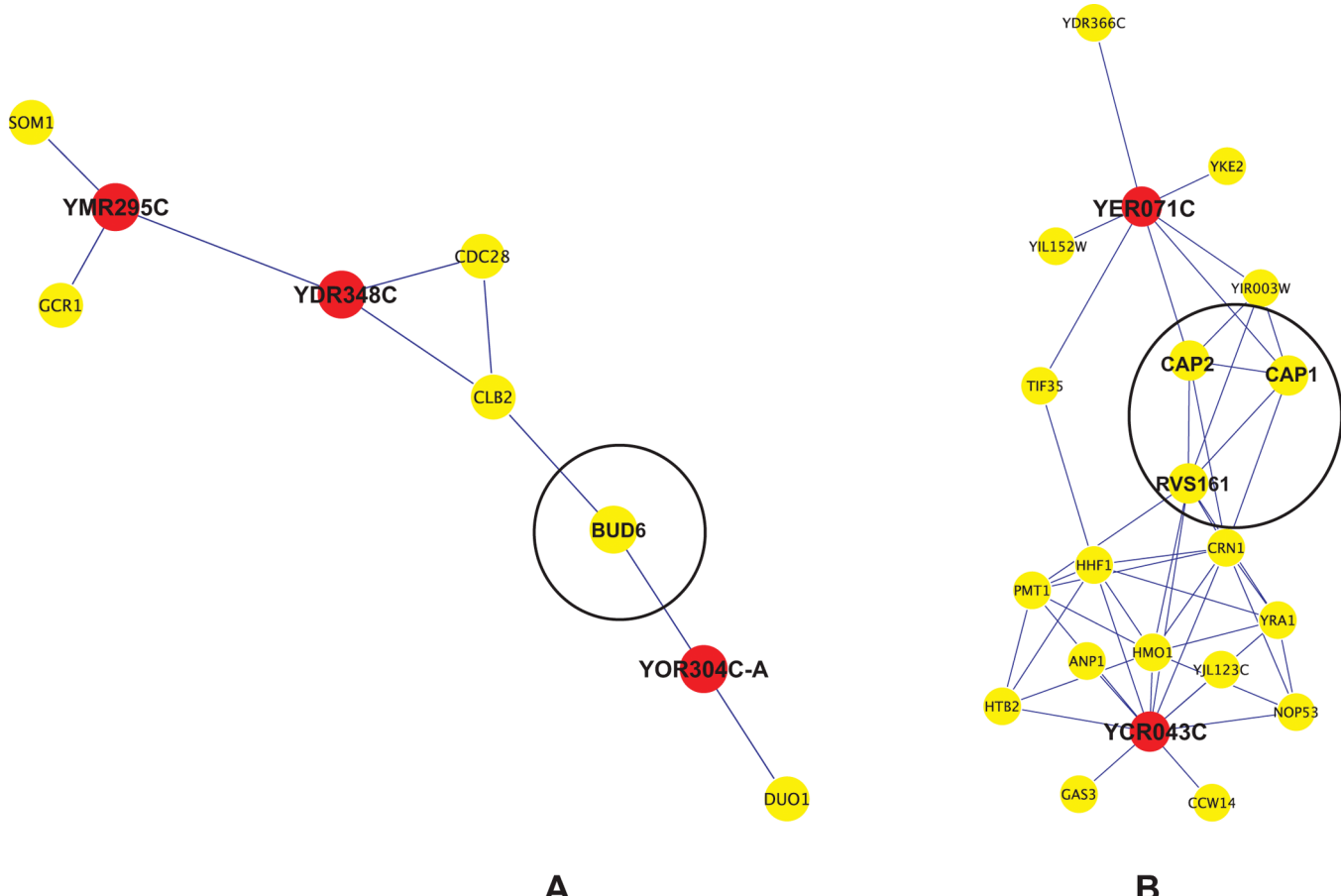


Figure 7. For uncharacterized proteins identified in the screen, some insights into their roles in polarized growth can be obtained from their functional associations in gene networks. The gene neighbors (yellow circles) of five uncharacterized proteins (red circles) in a functional gene network¹⁷ are plotted, indicating functional linkages by blue lines. Black circles enclose proteins already known to be part of the shmoos tip network. Panels A and B show two such uncharacterized sets of proteins that can be functionally tied via the network to different aspects of the shmoos tip gene network. In (A), Yor304C-a is functionally connected to BUD6 on the basis of evidence from affinity purification/mass spectrometry experiments summarized in the network. In (B), RVS161, CAP1 and CAP2, components of the known shmoos tip network, also connect to the uncharacterized genes, Yer071c and Ycr043c via protein complex data acquired by mass spectrometry.²⁷

processes very similar to and possibly mechanistically overlapping with shmoos formation. For example, Boi2 and Bni1 were conspicuously absent from the shmoos tip but were present at the bud tip and may reflect differential organization and positioning of the cytoskeletal architecture during pheromone induced mating as compared to vegetative buds.⁵⁰ In contrast, the formins Bni1 and Boi1 were found proximal to the shmoos tip consistent with their role in remodeling this dynamic locale.⁵¹

Additional proteins were found, emphasizing the differential sets of interactions driving the processes of mating and cell fusion. The shmoos tip marker Fus1¹² was recovered, as was Bck1, a cytosolic protein kinase in vegetative cells that appears to concentrate at the polarized shmoos tip. This is presumably due to its role in regulating cell wall integrity, a process closely connected to the mating response pathway.⁵² Similarly, Mid2, a cell wall sensor normally distributed uniformly around the cell wall⁹ shows a 3-fold increase in expression levels upon pheromone stimulation.⁵³ Its biased distribution around the shmoos tip is indicative of the increased occurrence of cell wall deposition at the site of polarized growth.⁵⁴

Yer071c, a protein annotated as having a punctate composite cytosolic localization, and Ycr043c, a Golgi annotated protein,⁹

were also recovered and have not been previously implicated in polarization. Some suggestions for more precise function can again be gained from the yeast functional network (Figure 7B), which connects Yer071c with actin cap binding proteins Cap1 and Cap2, while Ycr043c links to Rvs161, a lipid raft protein, all of which we observed at the shmoos tip. In addition, Car1, an arginase that when deleted causes cells to undergo G1 cell cycle arrest upon starvation⁵⁵ and Lsg1, a protein involved in 60S ribosome biogenesis are two other proteins we identified in this screen, but that were not obviously mating related. Our screen therefore adds evidence and provides putative hypotheses for the involvement of such uncharacterized proteins in the mating polarization pathway.

Conclusions

We report a large-scale imaging-based screen for proteins showing spatial localization to the growing tip of the yeast mating projection following pheromone response. A summary of our findings is presented in Figure 8. Our screen has enabled us to align the proteome down to the level of individual proteins identified along the polarization axis induced by pheromone stimulation. Upon the basis of this systematic

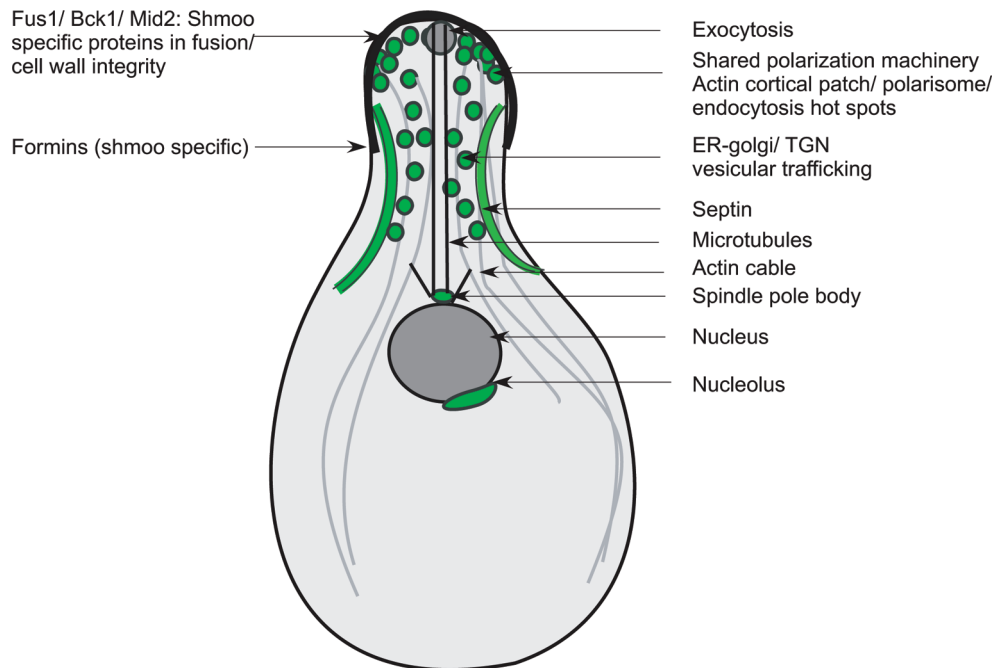


Figure 8. Schematic summarizing the spatial reorganization of organelles and protein complexes along the major polarization axis formed during shmooing. An alpha factor-induced polarization axis is established which leads to the spatial reorganization of multiple organelles in a roughly ordered fashion from proximal to the shmoo tip to the distal end of the cell. At the extreme growth tip lie proteins of exocytosis and mating, ringed by proteins associated with actin cortical patches and endocytosis, and—progressively moving away from the proximal tip—to the septins, spindle pole body, and nucleus, with the nucleolus generally oriented on the far side of the nucleus from the shmoo tip.

assay, we demonstrate that the bulk of shmoo-tip localized proteins are conserved with those localized to the bud tip during vegetative growth. These data therefore support a model for the adaptive reuse of polarized growth machinery between different polarized growth processes. For example, Huh et al.⁹ had shown that actin related genes are structured along the polarization axis during budding. We show that this observation is true during mating as well. This process is not automatic since the budding and mating projection sites are distinct and therefore the point of origin of cellular asymmetry is likely also different. Moreover, the 67 proteins shared between the mating and budding polarization processes (Figure 5) are significantly more conserved between human and yeast than expected by chance (39 of the 67 yeast genes have human orthologs,⁵⁶ $p < 0.023$, chi-square test), indicating that the functions of these core polarization components are likely to be preserved across eukaryotes. Although the process of establishment of cell polarity by proteins such as Cdc42, Cdc24 and Far1 are well-studied, the exact molecular mechanisms toward predictive cellular models are still wanting.⁵⁷ Our efforts are a first step toward screening proteome-wide dynamics to understand precisely how biological systems spatially coordinate protein interactions and regulate their dynamics.

Our screen recovered 37 proteins from the cell chip (out of 188 strains manually retested) and 37 from the classifier (out of 118 manually tested). This set had an overall intersection of 13 strains with the known set from SGD (Figure 5). A majority of known genes that this screen missed were low-abundance signaling proteins with signals too weak to be detected by GFP alone. In the 118 strains tested for the classifier, there were 81 false positives that did not localize to the shmoo tip. Of these 81, 18 were annotated to be bud localized and included bud specific formins such as Bnr1 and Boi2. Of the proteins

recovered in this screen, 7 were unique to shmoo tip. These findings, summarized in Figure 8, emphasize the involvement of a differential set of protein interactions driving each process toward their separate goals after the initial shared polarization machinery has been put in place.

Finally, this screen uncovers novel players in the polarization pathway. For example, proteins such as Ymr295c, Yor304c-a, and Ydr348c showed marked localization to the polarized growth tip in both budding and shmooing and thus likely represent conserved components of the general polarized growth pathway.

Acknowledgment. We thank Vishy Iyer for critical comments and help with array printing, Alice Zhao for help with imaging, and Erin O'Shea for the RFP-tagged organellar marker yeast strains. This work was supported by grants from the NIH (GM06779-01, GM076536-01), Welch Foundation (F1515, F1654), and a Packard Fellowship (E.M.M.).

References

- (1) Arimura, N.; Kaibuchi, K. Neuronal polarity: from extracellular signals to intracellular mechanisms. *Nat. Rev. Neurosci.* **2007**, *8* (3), 194–205.
- (2) Krummel, M. F.; Macara, I. Maintenance and modulation of T cell polarity. *Nat. Immunol.* **2006**, *7* (11), 1143–9.
- (3) Gaziava, I.; Bhat, K. M. Generating asymmetry: with and without self-renewal. *Prog. Mol. Subcell. Biol.* **2007**, *45*, 143–78.
- (4) Madden, K.; Snyder, M. Cell polarity and morphogenesis in budding yeast. *Annu. Rev. Microbiol.* **1998**, *52*, 687–744.
- (5) Dohlmam, H. G.; Thorner, J. W. Regulation of G protein-initiated signal transduction in yeast: paradigms and principles. *Annu. Rev. Biochem.* **2001**, *70*, 703–54.
- (6) Jarvik, J. W.; Fisher, G. W.; Shi, C.; Hennen, L.; Hauser, C.; Adler, S.; Berget, P. B. In vivo functional proteomics: mammalian genome annotation using CD-tagging. *BioTechniques* **2002**, *33* (4) 852–4, 856, 858–60 passim.

- (7) Hoffmann, C.; Gaietta, G.; Bunemann, M.; Adams, S. R.; Oberdorff-Maass, S.; Behr, B.; Vilardaga, J. P.; Tsien, R. Y.; Ellisman, M. H.; Lohse, M. J. A FLAsH-based FRET approach to determine G protein-coupled receptor activation in living cells. *Nat. Methods* **2005**, *2* (3), 171–6.
- (8) Kumar, A.; Agarwal, S.; Heyman, J. A.; Matson, S.; Heidtman, M.; Piccirillo, S.; Umansky, L.; Drawid, A.; Jansen, R.; Liu, Y.; Cheung, K. H.; Miller, P.; Gerstein, M.; Roeder, G. S.; Snyder, M. Subcellular localization of the yeast proteome. *Genes Dev.* **2002**, *16* (6), 707–19.
- (9) Huh, W. K.; Falvo, J. V.; Gerke, L. C.; Carroll, A. S.; Howson, R. W.; Weissman, J. S.; O'Shea, E. K. Global analysis of protein localization in budding yeast. *Nature* **2003**, *425* (6959), 686–91.
- (10) Narayanaswamy, R.; Niu, W.; Scouras, A. D.; Hart, G. T.; Davies, J.; Ellington, A. D.; Iyer, V. R.; Marcotte, E. M. Systematic profiling of cellular phenotypes with spotted cell microarrays reveals mating-pheromone response genes. *Genome Biol.* **2006**, *7* (1), R6.
- (11) Zhao, J.; Niu, W.; Yao, J.; Mohr, S.; Marcotte, E. M.; Lambowitz, A. M. Group II intron protein localization and insertion sites are affected by polyphosphate. *PLoS Biol.* **2008**, *6* (6), e150.
- (12) Proszynski, T. J.; Klemm, R.; Bagnat, M.; Gaus, K.; Simons, K. Plasma membrane polarization during mating in yeast cells. *J. Cell Biol.* **2006**, *173* (6), 861–6.
- (13) Kittler, J. a. I., J. Minimum error thresholding. *Pattern Recognit.* **1986**, *19*, 41–7.
- (14) Collins, T. J. ImageJ for microscopy. *BioTechniques* **2007**, *43* (1 Suppl), 25–30.
- (15) Frank, E.; Hall, M.; Trigg, L.; Holmes, G.; Witten, I. H. Data mining in bioinformatics using Weka. *Bioinformatics* **2004**, *20* (15), 2479–81.
- (16) Lee, I.; Date, S. V.; Adai, A. T.; Marcotte, E. M. A probabilistic functional network of yeast genes. *Science* **2004**, *306* (5701), 1555–8.
- (17) Lee, I.; Li, Z.; Marcotte, E. M. An improved, bias-reduced probabilistic functional gene network of baker's yeast, *Saccharomyces cerevisiae*. *PLoS One* **2007**, *2* (10), e988.
- (18) Baba, M.; Baba, N.; Ohsumi, Y.; Kanaya, K.; Osumi, M. Three-dimensional analysis of morphogenesis induced by mating pheromone alpha factor in *Saccharomyces cerevisiae*. *J. Cell Sci.* **1989**, *94* (Pt 2), 207–16.
- (19) Casolari, J. M.; Brown, C. R.; Drubin, D. A.; Rando, O. J.; Silver, P. A. Developmentally induced changes in transcriptional program alter spatial organization across chromosomes. *Genes Dev.* **2005**, *19* (10), 1188–98.
- (20) Newpher, T. M.; Smith, R. P.; Lemmon, V.; Lemmon, S. K. In vivo dynamics of clathrin and its adaptor-dependent recruitment to the Actin-based endocytic machinery in yeast. *Dev Cell* **2005**, *9* (1), 87–98.
- (21) Bagnat, M.; Simons, K. Cell surface polarization during yeast mating. *Proc. Natl. Acad. Sci. U.S.A.* **2002**, *99* (22), 14183–8.
- (22) Bidlingmaier, S.; Snyder, M. Large-scale identification of genes important for apical growth in *Saccharomyces cerevisiae* by directed allele replacement technology (DART) screening. *Funct. Integr. Genomics* **2002**, *1* (6), 345–56.
- (23) Changwei, Z.; Mingyong, X.; Ranran, W. Afr1p has a role in regulating the localization of Mpklp at the shmoo tip in *Saccharomyces cerevisiae*. *FEBS Lett.* **2007**, *581* (14), 2670–4.
- (24) Gehrung, S.; Snyder, M. The SPA2 gene of *Saccharomyces cerevisiae* is important for pheromone-induced morphogenesis and efficient mating. *J. Cell Biol.* **1990**, *111* (4), 1451–64.
- (25) Robinson, M. D.; Grigull, J.; Mohammad, N.; Hughes, T. R. FunSpec: a web-based cluster interpreter for yeast. *BMC Bioinf.* **2002**, *3*, 35.
- (26) Kumar, A.; des Etages, S. A.; Coelho, P. S.; Roeder, G. S.; Snyder, M. High-throughput methods for the large-scale analysis of gene function by transposon tagging. *Methods Enzymol.* **2000**, *328*, 550–74.
- (27) McGary, K. L.; Lee, I.; Marcotte, E. M. Broad network-based predictability of *Saccharomyces cerevisiae* gene loss-of-function phenotypes. *Genome Biol.* **2007**, *8* (12), R258.
- (28) Reimand, J.; Kull, M.; Peterson, H.; Hansen, J.; Vilo, J. gProfilier--a web-based toolset for functional profiling of gene lists from large-scale experiments. *Nucleic Acids Res.* **2007**, *35* (Web Server issue), W193–200.
- (29) He, B.; Xi, F.; Zhang, X.; Zhang, J.; Guo, W. Exo70 interacts with phospholipids and mediates the targeting of the exocyst to the plasma membrane. *EMBO J.* **2007**, *26* (18), 4053–65.
- (30) Wiederkehr, A.; Du, Y.; Pypaert, M.; Ferro-Novick, S.; Novick, P. Sec3p is needed for the spatial regulation of secretion and for the inheritance of the cortical endoplasmic reticulum. *Mol. Biol. Cell* **2003**, *14* (12), 4770–82.
- (31) Finger, F. P.; Hughes, T. E.; Novick, P. Sec3p is a spatial landmark for polarized secretion in budding yeast. *Cell* **1998**, *92* (4), 559–71.
- (32) Pruyne, D.; Legesse-Miller, A.; Gao, L.; Dong, Y.; Bretscher, A. Mechanisms of polarized growth and organelle segregation in yeast. *Annu. Rev. Cell. Dev. Biol.* **2004**, *20*, 559–91.
- (33) Huckaba, T. M.; Gay, A. C.; Pantalena, L. F.; Yang, H. C.; Pon, L. A. Live cell imaging of the assembly, disassembly, and Actin cable-dependent movement of endosomes and Actin patches in the budding yeast, *Saccharomyces cerevisiae*. *J. Cell Biol.* **2004**, *167* (3), 519–30.
- (34) Palmgren, S.; Ojala, P. J.; Wear, M. A.; Cooper, J. A.; Lappalainen, P. Interactions with PIP2, ADP-Actin monomers, and capping protein regulate the activity and localization of yeast twinfilin. *J. Cell Biol.* **2001**, *155* (2), 251–60.
- (35) Clark, M. G.; Teply, J.; Haarer, B. K.; Viggiano, S. C.; Sept, D.; Amberg, D. C. A genetic dissection of Aip1p's interactions leads to a model for Aip1p-cofilin cooperative activities. *Mol. Biol. Cell* **2006**, *17* (4), 1971–84.
- (36) Cope, M. J.; Yang, S.; Shang, C.; Drubin, D. G. Novel protein kinases Ark1p and Prk1p associate with and regulate the cortical actin cytoskeleton in budding yeast. *J. Cell Biol.* **1999**, *144* (6), 1203–18.
- (37) Smythe, E.; Ayscough, K. R. The Ark1/Prk1 family of protein kinases. Regulators of endocytosis and the Actin skeleton. *EMBO Rep.* **2003**, *4* (3), 246–51.
- (38) Tang, H. Y.; Xu, J.; Cai, M. Pan1p, End3p, and S1a1p, three yeast proteins required for normal cortical Actin cytoskeleton organization, associate with each other and play essential roles in cell wall morphogenesis. *Mol. Cell. Biol.* **2000**, *20* (1), 12–25.
- (39) Bertling, E.; Quintero-Monzon, O.; Mattila, P. K.; Goode, B. L.; Lappalainen, P. Mechanism and biological role of profilin-Srv2/CAP interaction. *J. Cell Sci.* **2007**, *120* (Pt 7), 1225–34.
- (40) Dewar, H.; Warren, D. T.; Gardiner, F. C.; Gourlay, C. G.; Satish, N.; Richardson, M. R.; Andrews, P. D.; Ayscough, K. R. Novel proteins linking the actin cytoskeleton to the endocytic machinery in *Saccharomyces cerevisiae*. *Mol. Biol. Cell* **2002**, *13* (10), 3646–61.
- (41) Warren, D. T.; Andrews, P. D.; Gourlay, C. W.; Ayscough, K. R. Sla1p couples the yeast endocytic machinery to proteins regulating actin dynamics. *J. Cell Sci.* **2002**, *115* (Pt 8), 1703–15.
- (42) Gilstring, C. F.; Melin-Larsson, M.; Ljungdahl, P. O. Shr3p mediates specific COPII coatomer-cargo interactions required for the packaging of amino acid permeases into ER-derived transport vesicles. *Mol. Biol. Cell* **1999**, *10* (11), 3549–65.
- (43) Peng, R.; De Antoni, A.; Gallwitz, D. Evidence for overlapping and distinct functions in protein transport of coat protein Sec24p family members. *J. Biol. Chem.* **2000**, *275* (15), 11521–8.
- (44) Grote, E.; Carr, C. M.; Novick, P. J. Ordering the final events in yeast exocytosis. *J. Cell Biol.* **2000**, *151* (2), 439–52.
- (45) Wicky, S.; Frischmuth, S.; Singer-Kruger, B. Bsp1p/Ypr171p is an adapter that directly links some synaptojanin family members to the cortical actin cytoskeleton in yeast. *FEBS Lett.* **2003**, *537* (1–3), 35–41.
- (46) Pashkova, N.; Catlett, N. L.; Novak, J. L.; Wu, G.; Lu, R.; Cohen, R. E.; Weisman, L. S. Myosin V attachment to cargo requires the tight association of two functional subdomains. *J. Cell Biol.* **2005**, *168* (3), 359–64.
- (47) Medkova, M.; France, Y. E.; Coleman, J.; Novick, P. The rab exchange factor Sec2p reversibly associates with the exocyst. *Mol. Biol. Cell* **2006**, *17* (6), 2757–69.
- (48) Walther, T. C.; Brickner, J. H.; Aguilar, P. S.; Bernales, S.; Pantoja, C.; Walter, P. Eisosomes mark static sites of endocytosis. *Nature* **2006**, *439* (7079), 998–1003.
- (49) Fleischer, T. C.; Weaver, C. M.; McAfee, K. J.; Jennings, J. L.; Link, A. J. Systematic identification and functional screens of uncharacterized proteins associated with eukaryotic ribosomal complexes. *Genes Dev.* **2006**, *20* (10), 1294–307.
- (50) Butterly, S. M.; Yoshida, S.; Pellman, D. Yeast formins Bnl1 and Bnr1 utilize different modes of cortical interaction during the assembly of actin cables. *Mol. Biol. Cell* **2007**, *18* (5), 1826–38.
- (51) Cabib, E.; Drgonova, J.; Drgon, T. Role of small G proteins in yeast cell polarization and wall biosynthesis. *Annu. Rev. Biochem.* **1998**, *67*, 307–33.
- (52) Buehrer, B. M.; Errede, B. Coordination of the mating and cell integrity mitogen-activated protein kinase pathways in *Saccharomyces cerevisiae*. *Mol. Cell. Biol.* **1997**, *17* (11), 6517–25.
- (53) Ono, T.; Suzuki, T.; Anraku, Y.; Iida, H. The MID2 gene encodes a putative integral membrane protein with a Ca(2+)-binding domain and shows mating pheromone-stimulated expression in *Saccharomyces cerevisiae*. *Gene* **1994**, *151* (1–2), 203–8.
- (54) Lommel, M.; Bagnat, M.; Strahl, S. Aberrant processing of the WSC family and Mid2p cell surface sensors results in cell death of *Saccharomyces cerevisiae* O-mannosylation mutants. *Mol. Cell. Biol.* **2004**, *24* (1), 46–57.

- (55) Cooper, T. G.; Britton, C.; Brand, L.; Sumrada, R. Addition of basic amino acids prevents G-1 arrest of nitrogen-starved cultures of *Saccharomyces cerevisiae*. *J. Bacteriol.* **1979**, *137* (3), 1447–8.
- (56) Berglund, A. C.; Sjolund, E.; Ostlund, G.; Sonnhammer, E. L. InParanoid 6: eukaryotic ortholog clusters with inparalogs. *Nucleic Acids Res.* **2008**, *36* (Database issue), D263–6.
- (57) Marco, E.; Wedlich-Soldner, R.; Li, R.; Altschuler, S. J.; Wu, L. F. Endocytosis optimizes the dynamic localization of membrane proteins that regulate cortical polarity. *Cell* **2007**, *129* (2), 411–22.

PR800524G